ISSN 1063-7834, Physics of the Solid State, 2015, Vol. 57, No. 5, pp. 1014–1022. © Pleiades Publishing, Ltd., 2015.
Original Russian Text © V.G. Myagkov, L.E. Bykova, V.S. Zhigalov, I.A. Tambasov, G.N. Bondarenko, A.A. Matsynin, A.N. Rybakova, 2015, published in Fizika Tverdogo Tela, 2015, Vol. 57, No. 5, pp. 999–1006.

LOW-DIMENSIONAL SYSTEMS

Solid-State Synthesis, Structural and Magnetic Properties of CoPd Films

V. G. Myagkov[a, *], L. E. Bykova[a], V. S. Zhigalov[a], I. A. Tambasov[a], G. N. Bondarenko[b], A. A. Matsynin[a], and A. N. Rybakova[a]

[a] *Kirensky Institute of Physics, Siberian Branch of the Russian Academy of Sciences, Akademgorodok 50–38, Krasnoyarsk, 660036 Russia*

[b] *Institute of Chemistry and Chemical Technology, Siberian Branch of the Russian Academy of Sciences, Alademgorodok 50–24, Krasnoyarsk, 660036 Russian*

* *e-mail: miagkov@iph.krasn.ru*

Received November 24, 2014

Abstract—The results of the investigation of the structural and magnetic properties of CoPd films with equiatomic composition have been presented. The films have been synthesized by vacuum annealing of polycrystalline Pd/Co and epitaxial Pd/α-Co(110) and Pd/β-Co(001) bilayer samples. It has been shown that, for all samples, the annealing to 400°C does not lead to the mixing of layers and the formation of compounds. A further increase in the annealing temperature results in the formation of a disordered CoPd phase at the Pd/Co interface, which is fully completed after annealing at 650°C. The epitaxial relationships between the disordered CoPd phase and the MgO(001) substrate are determined as follows: CoPd(110)$\langle \bar{1}11 \rangle$ || MgO(001)⟨100⟩ and CoPd(001)[100] || MgO(001)[100], which are formed in the Pd/α-Co(110) and Pd/β-Co(001) films, respectively. According to the calculations, the first magnetocrystalline anisotropy constants of the disordered CoPd phase for Pd/α-Co(110) and Pd/β-Co(001) samples have close values: $K_1^{\mathrm{CoPd}} = -(1.6 \pm 0.4) \times 10^5$ erg/cm^3. A possible mechanism of the solid-state synthesis of the CoPd alloy is proposed.

DOI: 10.1134/S1063783415050236

1. INTRODUCTION

Multilayers with perpendicular magnetic anisotropy have continued to attract attention of researchers and have been intensively investigated for the purpose to use in practice as media for perpendicular recording [1, 2] and random-access memory devices [3]. Multilayer Co/Pd samples have a perpendicular magnetic anisotropy of ~8×10^6 erg/cm^3 [4], which is slightly less than in materials with high uniaxial magnetocrystalline anisotropy [5]. Experimental observations revealed that heating to ~400°C does not change the magnetic properties of Co/Pd multilayers. However, annealing at temperatures higher than 400°C leads to a degradation of the perpendicular magnetic anisotropy, and the easy magnetization direction becomes aligned with the sample plane. This is interpreted by assuming that the heating is responsible for the mixing and alloying at the initially sharp Pd/Co interface [6–10]. The chemical mixing at the Co/Pd interface is observed upon ion implantation [11] and intense laser irradiation, which lead to a decrease in the perpendicular magnetic anisotropy [12, 13]. This agrees with the calculations of the electronic structure, which predict a decrease in the perpendicular magnetic anisotropy due to the formation of defects and alloying at the Co/Pd interface [14]. According to the phase equilibrium diagram, in the Co–Pd system, there is only a disordered Co_xPd_{1-x} solid solution with a lattice constant that varies depending on the composition from $a = 0.3826$ nm for Pd to $a = 0.3544$ nm for β-Co. However, the metastable ordered phases $L1_0$-CoPd and $L1_2$-$CoPd_3$ with the order–disorder transition temperatures of ~830°C were revealed in Co_xPd_{1-x} alloy thin films prepared by vacuum deposition [10, 15].

Currently, there are few publications devoted to the study of conditions for the formation of disordered Co_xPd_{1-x} solid solutions and there are no data on their magnetic properties both for bulk samples and for thin films. Important information about the conditions for the formation and ordering of CoPd phases during annealings can be obtained from the investigation of solid-state reactions between thin-film reactants Co and Pd.

It is well known that solid-state reactions in thin films start at a specific temperature (initiation temperature T_{in}) with the formation of only one phase, which is referred to as the first phase [16–18]. A further increase in the temperature leads to the appearance of other phases, which form a phase sequence. Until now, no unique explanation has been proposed for the formation of the first phase and phase sequence among many phases of the given binary system, and no

determination has been offered for their initiation temperature, although some models have been proposed [16–18].

In this work, we have investigated the solid-state reactions between the Pd film and polycrystalline Co film, as well as the structures with hexagonal α-Co(110) and cubic β-Co(001) epitaxial layers during annealing in vacuum. It has been shown that, regardless of the structural modification and the crystalline state of cobalt in samples of the 1Co : 1Pd composition, an increase in the annealing temperature above 400°C leads to the onset of the mixing of Co and Pd layers and the formation of the disordered CoPd phase.

2. SAMPLE PREPARATION AND EXPERIMENTAL TECHNIQUE

The initial polycrystalline Pd/Co films and initial epitaxial Pd/α-Co(110)/MgO(001) and Pd/β-Co(001)/MgO(001) films were prepared by sequential vacuum deposition of Co and Pd layers on glass and MgO(001) substrates, respectively. Before the deposition, the substrates were outgassed at 400°C for 1 h. The experiments were carried out using samples with an atomic ratio of 1Co : 1Pd (hereinafter, CoPd) and a total thickness of 300 nm. The deposition of a Co layer in a vacuum chamber with a pressure of 10^{-6} mbar at a temperature of 250–300°C led to the epitaxial growth of α-Co(110) on MgO(001). However, the deposition in vacuum with a pressure of 10^{-5} mbar at a temperature of the MgO(001) substrate in the range of 250–300°C resulted predominantly in the formation of an epitaxial cubic β-Co(001) layer. The magnetic anisotropy was measured on a rotating sample magnetometer with a maximum magnetic field of 18 kOe. The X-ray fluorescence analysis was used to determine the thicknesses of the Co and Pd layers. The formed phases were identified on a DRON-4-07 (CuK_α radiation). X-ray diffraction investigations of the epitaxial orientation of the phases were performed on a PANalytical X'Pert PRO diffractometer with a PIXcel solid-state detector. The initial samples of Pd/Co, Pd/α-Co(110)/MgO(001), and Pd/β-Co(001)/MgO(001) were subjected to thermal annealing in a vacuum of 10^{-6} mbar at temperatures in the range from 250 to 650°C with a step of 50°C and exposure at each temperature for 30 min. All the measurements were performed at room temperature. The temperature dependence of the electrical resistance during the synthesis of the disordered CoPd phase upon heating of polycrystalline Pd/Co films was measured by the four-point probe method with clamping contacts in a vacuum of 10^{-6} mbar at a heating rate of ~5°C/min.

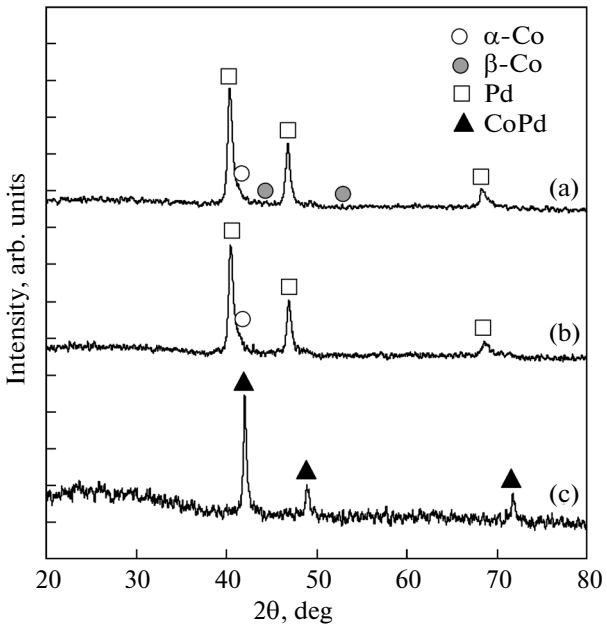

Fig. 1. X-ray diffraction patterns of the polycrystalline Pd/Co film sample at annealing temperatures of (a) 20, (b) 400, and (c) 500°C.

3. EXPERIMENTAL RESULTS AND DISCUSSION

3.1. Solid-State Synthesis of the CoPd Alloy in Polycrystalline Pd/Co Films

The X-ray diffraction patterns of the initial polycrystalline Pd/Co films deposited on glass substrates contained reflections from Pd and α-Co, as well as weak peaks of the β-Co phases (Fig. 1a), which did not change upon annealing to 400°C (Fig. 1b). Therefore, the initial Co layer contained a mixture of crystallites of the low-temperature (α-Co) and high-temperature (β-Co) phases. After annealing at 500°C, the reflections from Pd and Co disappeared and reflections appeared from a compound with the lattice parameter $a = 0.372$ nm, which corresponds to the $Co_{50}Pd_{50}$ solid solution (Fig. 1c). This indicates that the mixing of Co and Pd layers and the synthesis of the disordered CoPd alloy have the initiation temperature above 400°C. Figure 2 shows the dependence of the electrical resistance of the initial Pd/Co films on the heating temperature. With an increase in the temperature, the electrical resistance increases monotonically, following the metallic behavior of the temperature dependence of the electrical resistance of the reactants. A sharp increase in the resistance above 400°C certainly indicates the mixing of Co and Pd layers and the synthesis of the CoPd alloy with the initiation temperature T_{in} ~ 400°C.

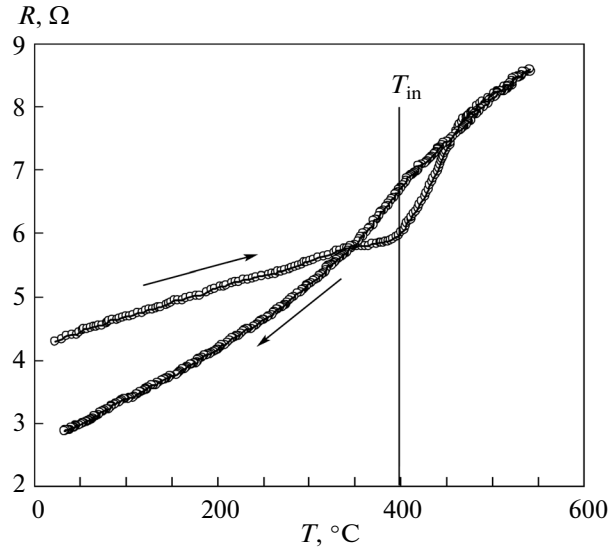

Fig. 2. Dependence of the electrical resistance R of the polycrystalline Pd/Co film sample on the temperature T. The arrows indicate the direct and reverse runs. A sharp increase in the electrical resistance R begins at the initiation temperature $T_{in} = 400$°C of the solid-state reaction between the Pd and Co films.

3.2. Solid-State Synthesis of the CoPd Alloy in Epitaxial Pd/α-Co(110) Films

The initial Pd/α-Co(110) films were formed by deposition of a Pd layer on the α-Co(110)/MgO(001) surface in a vacuum of 10^{-6} mbar at a temperature of ~250°C. Figure 3a shows the X-ray diffraction pattern of the initial Pd/α-Co(110) film formed on the MgO(001) surface, which contains a strong peak of α-Co(110) and a weak reflection from Pd(002). This suggests the growth of a finely dispersed Pd layer on the α-Co(110) surface. The analysis performed in [19] revealed that α-Co(110) crystallites grow on MgO(001) in accordance with the two epitaxial relationships

$$\begin{aligned}&\alpha\text{-Co}(110)[001] \parallel \text{MgO}(001)[110],\\ &\alpha\text{-Co}(110)[100] \parallel \text{MgO}(001)[1\bar{1}0].\end{aligned} \quad (1)$$

These relationships also hold for the growth of α-Co(110) crystallites on GaAs(001) [20] and bilayer Co/V films on MgO(001), which were prepared in an ultrahigh vacuum [21]. The magnetic anisotropy energy E_K of the hexagonal crystal (without taking into account the anisotropy in the basal plane) has the form $E_K^{\alpha\text{-Co}} = K_1^{\alpha\text{-Co}}\sin^2\varphi + K_2^{\alpha\text{-Co}}\sin^4\varphi$, ..., where φ is the angle between the **c** axis and the direction of magnetization M_S [22]. For α-Co, the magnetocrystalline anisotropy constants are $K_1^{\alpha\text{-Co}} = +4.3 \times 10^6$ erg/cm^3 and $K_2^{\alpha\text{-Co}} = +1.2 \times 10^6$ erg/cm^3 [22].

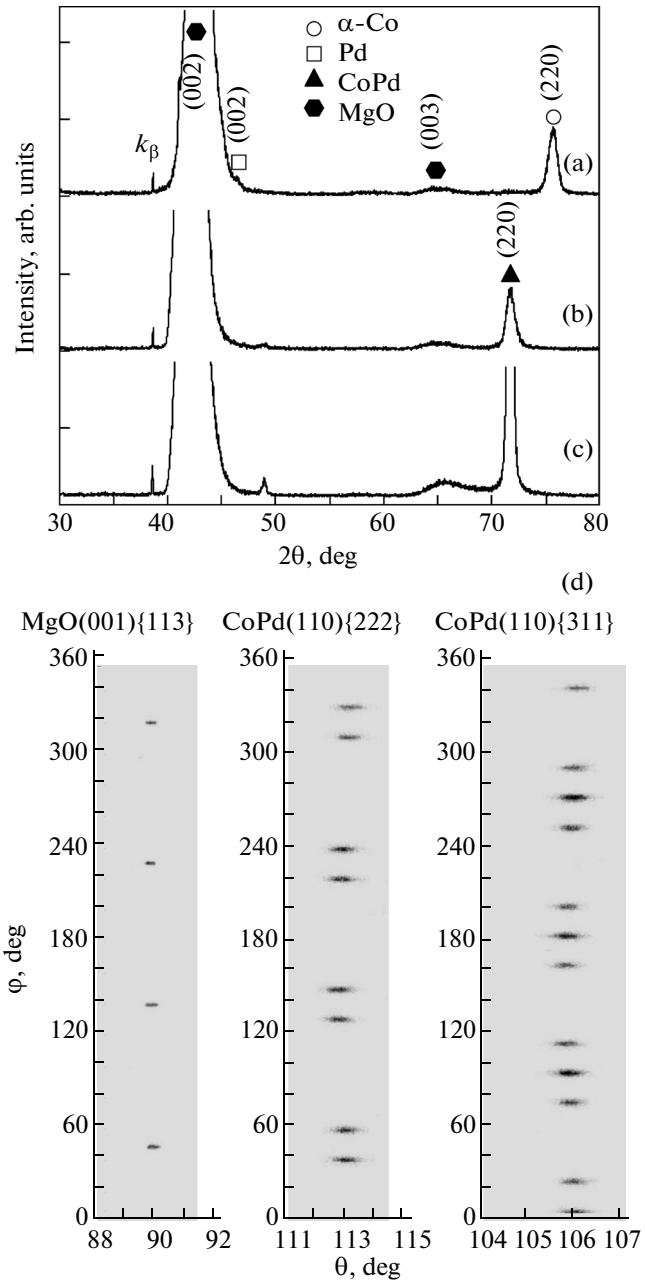

Fig. 3. (a–c) X-ray diffraction patterns of the Pd/α-Co(110) films at annealing temperatures of (a) 20, (b) 500, and (c) 650°C. (d) Asymmetric diffraction image (φ–2θ) for the MgO(001) substrate and CoPd(110) films after annealing at 650°C. These scans show the epitaxial growth CoPd(110)⟨$\bar{1}$11⟩ || MgO(001)⟨100⟩.

Under the assumption that the α-Co(110) crystallites growing with orientations of the axis along the [110] and [$\bar{1}$10] directions of MgO and satisfying relationship (1) are exchange-related and have equal volumes, their effective magnetic constant $K^{\alpha\text{-Co}(110)}$ is equal to the second magnetocrystalline anisotropy constant $K_2^{\alpha\text{-Co}}$ of the α-Co phase ($K^{\alpha\text{-Co}(110)} = K_2^{\alpha\text{-Co}}$)

[20]. The coincidence of the experimental values of $K^{\alpha\text{-Co}(110)}$ and $K_2^{\alpha\text{-Co}}$ confirms the epitaxial growth of α-Co(110) crystallites on MgO(001) according to the epitaxial relationships (1). The easy magnetization axes of the α-Co(110) films coincide with the [110] and $[1\bar{1}0]$ directions of the MgO(001) substrate. In the coordinate system related to the [100] and $[0\bar{1}0]$ axes of the MgO(001) substrate, the constant $K^{\alpha\text{-Co}(110)}$ has a negative value. Figure 4a shows the schematic drawing of the α-Co(110) crystallites grown on MgO(001) in accordance with the epitaxial relationships (1).

The diffraction patterns of the initial Pd/α-Co(110) samples did not change up to 400°C. The annealing at 500°C leads to a decrease in the peaks of the α-Co(110) phase and to the onset of formation of a new strong (110) peak of the CoPd phase (Fig. 3b). With an increase in the annealing temperature to 650°C, the (110) reflection significantly increases due to both an increase in the volume and an increase in the crystalline perfection of crystallites of the CoPd(110) phase (Fig. 3c). The epitaxial relationship in the plane between the CoPd(110) film and the MgO(001) substrate

$$\text{CoPd}(110)\langle\bar{1}11\rangle \parallel \text{MgO}(001)\langle 100\rangle \qquad (2)$$

was determined by measuring the asymmetric φ-scans of the {222} and {311} reflections from the CoPd phase and the {113} reflection from the MgO substrate (Fig. 3d).

Figure 4b shows the schematic diagram of four variants of the CoPd(110) crystallites synthesized on the MgO(001) surface after annealing at 650°C, which satisfy the epitaxial relationship (2). It can be seen that the initial α-Co(110) crystallites grown on the MgO(001) surface, which satisfy the epitaxial relationships (1) (Fig. 4a), after the reaction with Pd form CoPd(110) crystallites in accordance with the epitaxial relationship (2) (Fig. 4b).

3.3. Solid-State Synthesis of the CoPd Alloy in Epitaxial Pd/β-Co(001) Films

The epitaxial β-Co(001) layer was formed by deposition of cobalt on the MgO(001) substrate at a temperature of ~250°C in a vacuum of 10^{-5} mbar. Previously, it was shown that the high-temperature metastable cubic phase β-Co is formed under these deposition conditions [23] and in an ultrahigh vacuum [24, 25]. The β-Co films had the preferred (001) orientation and biaxial magnetic anisotropy with the constant coinciding with the first magnetocrystalline anisotropy constant of cubic cobalt $K_1^{\beta\text{-Co}(110)} = -(5.5\text{–}6.0) \times 10^5$ erg/cm^3 [26–28]. The easy magnetization axes of the β-Co film coincided with the [110] and $[1\bar{1}0]$ directions of the MgO(001) substrate. This confirms the existence of the following orientation relationship for the epitaxial growth of cubic cobalt on the MgO(001) surface:

$$\beta\text{-Co}(001)[100] \parallel \text{MgO}(001)[100]. \qquad (3)$$

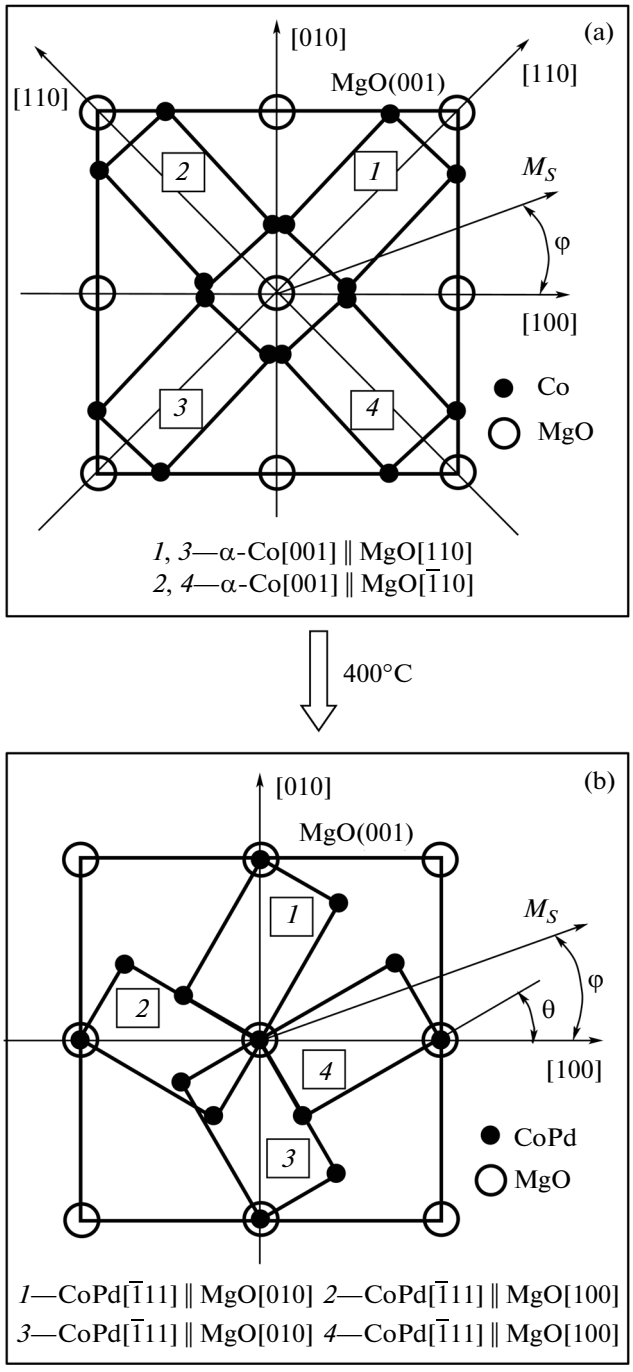

Fig. 4. Schematic diagrams showing the structural transformation on the MgO(001) surface for (a) initial α-Co(110) crystallites and (b) crystallites after the solid-state reaction with Pd.

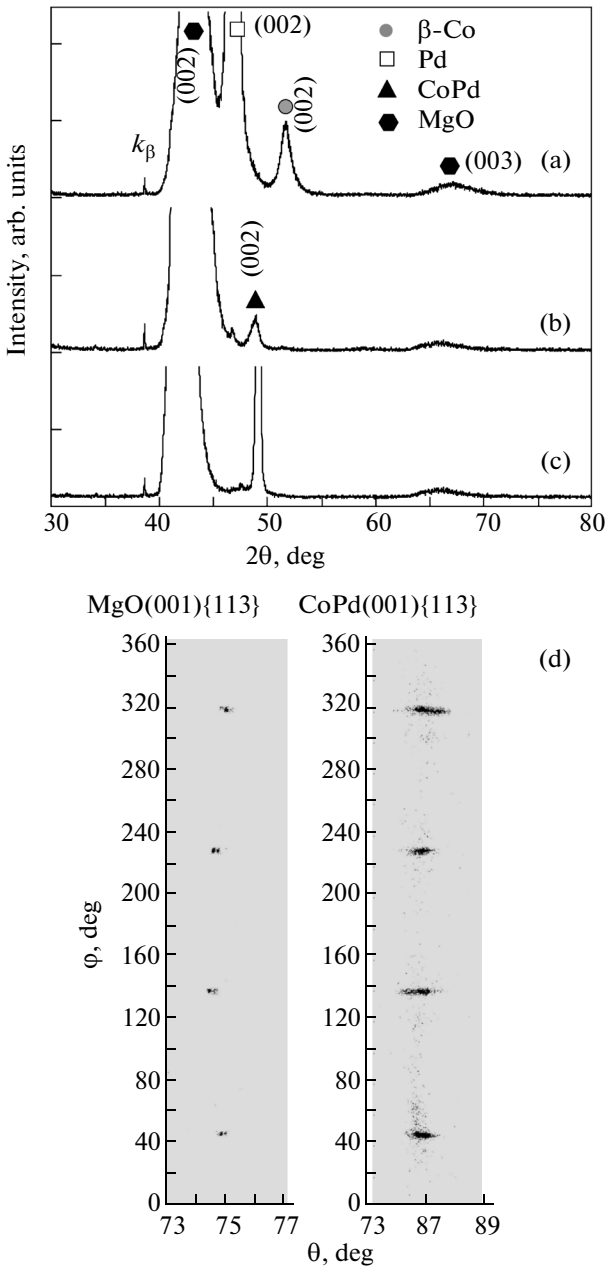

Fig. 5. (a–c) X-ray diffraction patterns of the Pd/β-Co(001) films at annealing temperatures of (a) 20, (b) 500, and (c) 650°C. (d) Asymmetric diffraction image (φ–2θ) for the MgO(001) substrate and CoPd(001) films after annealing at 650°C. These scans show the epitaxial growth CoPd(001)[100] || MgO(001)[100].

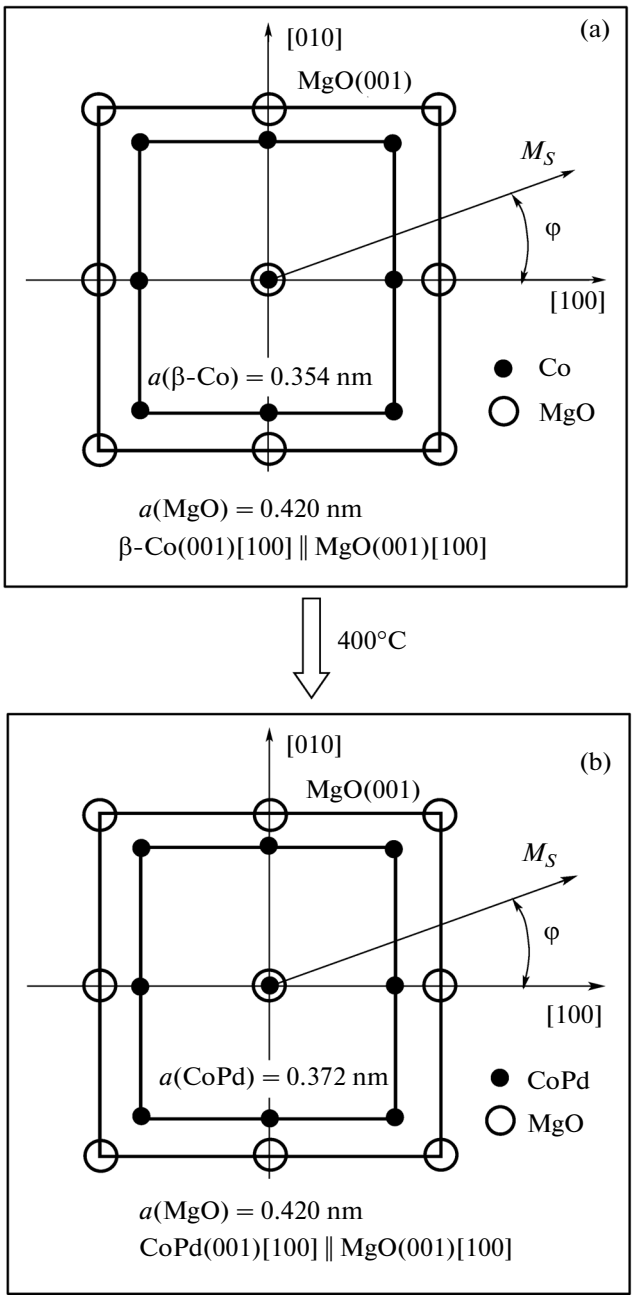

Fig. 6. Schematic diagrams showing the structural transformation on the MgO(001) surface for (a) initial crystallites β-Co(001) and (b) crystallites after the solid-state reaction with Pd.

The deposition of the Pd layer was performed at a temperature of ~250°C and did not change the magnetic properties of the β-Co layer. The only Pd(002) peak in the X-ray diffraction pattern confirms the successive preferential formation of the epitaxial β-Co(001) and Pd(001) layers on the MgO(001) surface (Fig. 5a). Figure 6a shows the schematic diagram of the growth of β-Co(001) crystallites on the MgO(001) surface, which satisfy the epitaxial relationship (3).

The X-ray diffraction patterns of the initial Pd (001)/β-Co(001) samples did not change up to 400°C. After annealing at 500°C, the peaks of Pd(002) and β-Co(002) significantly decreased and new (002) reflections from the CoPd phase appeared (Fig. 5b). With a further increase in the annealing temperature to 650°C, the reflections from CoPd (002) significantly

increased and the peaks from Pd(002) and β-Co(002) completely disappeared (Fig. 5c). This suggests the completion of the synthesis of CoPd(001) crystallites, which inherit the (001) orientation of the initial β-Co(001) films. The absence of the superstructure (001) reflection confirms that the formed CoPd phase is disordered. Using the asymmetric scanning of the {113} reflections, we determined the following epitaxial relationship for synthesized CoPd(001) crystallites on the MgO(001) substrate after annealing at 650°C (Fig. 5d):

$$\text{CoPd}(001)[100] \parallel \text{MgO}(001)[100], \quad (4)$$

their schematic drawing is shown in Fig. 6b. The same epitaxial relationship (4) holds for the disordered CoPd(001) phases formed under different deposition conditions on the MgO(001) substrate [29, 30]. Using the peak of CoPd(002), we determined the lattice parameter of the CoPd phase $a = 0.37135(4)$ nm, which is close to the value for bulk CoPd alloy samples.

3.4. Evolution of the Magnetocrystalline Anisotropy in Epitaxial Pd/α-Co(110) and Pd/β-Co(001) Films

The in-plane biaxial magnetic anisotropy constants $K^{\text{Pd}/\alpha\text{-Co}(110)}$ and $K^{\text{Pd}/\beta\text{-Co}(001)}$ of the initial films Pd/α-Co(110) and Pd/β-Co(001) containing crystallites shown in Figs. 4a and 6a are equal to the magnetocrystalline anisotropy constants $K_2^{\alpha\text{-Co}}$ and $K_1^{\beta\text{-Co}}$, respectively. Figure 7 shows the dependences of the effective magnetic anisotropy constants $K_{\text{eff}}^{110} = K^{\text{Pd}/\alpha\text{-Co}(110)}/K_2^{\alpha\text{-Co}}$ and $K_{\text{eff}}^{001} = K^{\text{Pd}/\beta\text{-Co}(001)}/K_1^{\beta\text{-Co}}$ on the annealing temperature T for the Pd/α-Co(110) and Pd/β-Co(001) samples, respectively.

Within the experimental error, up to the temperature of 400°C, the anisotropy constants $K_{\text{eff}}^{110}(T)$ (Fig. 7a) and $K_{\text{eff}}^{001}(T)$ (Fig. 7b) did not depend on the annealing temperature T. At annealing temperatures above 400°C, the observed decrease in the absolute values of the constants K_{eff}^{110} (Fig. 7a) and K_{eff}^{001} (Fig. 7b) as a function of the annealing temperature T is associated with the onset of the mixing of Pd and Co layers and with the synthesis of the CoPd phase. This agrees with the data on the electrical resistance (Fig. 2) and X-ray diffraction (Figs. 1, 3, 5), according to which the initiation temperature of the reaction of palladium with cobalt is $T_{\text{in}} \sim 400$°C. As was shown above, after annealing at 650°C, the reaction between Pd and Co is fully completed and, in the Pd/α-Co(110) films, four variants of CoPd(110) crystallites are formed (Fig. 4b), which grow on the MgO(001) surface and satisfy the epitaxial relationship (2). It is also known that four variants of Fe(110) crystallites grow on Cu(001) in accordance with the Pietsch epitaxial relationship $\text{Fe}(110)\langle\bar{1}11\rangle \parallel \text{Cu}(001)\langle 110\rangle$ [31–37]. The magnetic anisotropy energy density $E(\varphi)$ of exchange-coupled CoPd(110) crystallites satisfying the epitaxial relationship (2) is described by the expression similar to that obtained for Fe(110) crystallites satisfying the Pietsch relationship [37]:

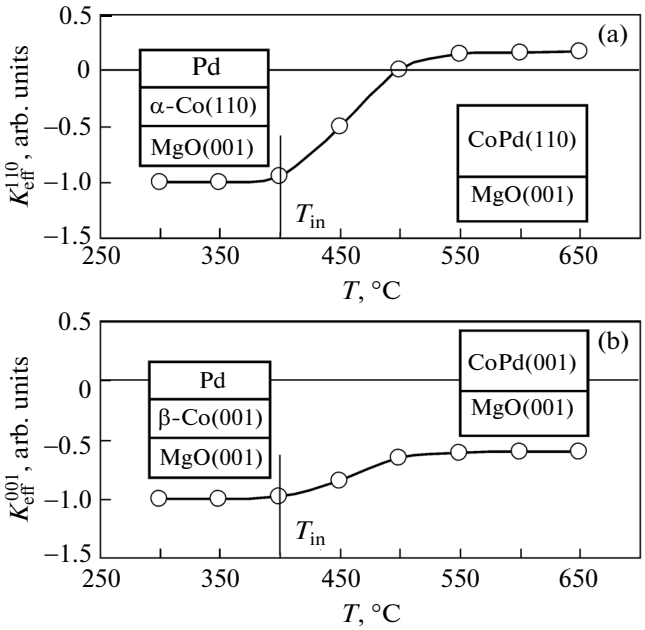

Fig. 7. Dependences of the magnetic anisotropy constants (a) K_{eff}^{110} and (b) K_{eff}^{001} on the annealing temperature T and schematic diagrams for the Pd/α-Co(110) and Pd/β-Co(001) films, respectively. Changes in the values of K_{eff}^{110} and K_{eff}^{001} begin at the initiation temperature $T_{\text{in}} \sim 400$°C of the solid-state reaction between the Co and Pd films and are completed at a temperature of ~650°C.

$$\begin{aligned} E(\varphi) &= K^{\text{CoPd}(110)} \sin^2\varphi\cos^2\varphi \\ &= (3/4)K_1^{\text{CoPd}}\cos 4\theta \sin^2\varphi\cos^2\varphi, \end{aligned} \quad (5)$$

where φ is the angle between the magnetization M_S and the [100] direction of MgO and θ is the angle of misorientation of CoPd(110) crystallites with respect to the [100] and [010] directions of MgO(001) (Fig. 4b). From expression (5), it follows that the biaxial magnetocrystalline anisotropy constant $K^{\text{CoPd}(110)}$ of the CoPd(110) crystallites satisfying the epitaxial relationship (2) (Fig. 4b) is determined by the first magnetocrystalline anisotropy constant K_1^{CoPd} of the CoPd alloy:

$$K^{\text{CoPd}(110)} = (3/4)K_1^{\text{CoPd}}\cos 4\theta. \quad (6)$$

For the CoPd(110) crystallites satisfying the epitaxial relationship (3), we have the angle $\theta = 35.25°$ (Fig. 4b). By substituting the experimental value of

$K_{\text{eff}}^{\text{Pd}/\alpha\text{-Co}}$ (T = 650°C) = $K^{\text{Co}(110)}$ = +(1.0 ± 0.4) × 10^5 erg/cm^3 (Fig. 7a) and $\theta \cong 35.25°$ (Fig. 4b) into expression (6) and taking into account the ratio of the Pd film volume to the Co film volume (1 : 3), we obtain the first magnetocrystalline anisotropy constant $K_1^{\text{CoPd}} = -(1.6 \pm 0.4) \times 10^5$ erg/cm^3 for the CoPd alloy. It is important to note that, according to expression (6), the constants $K^{\text{CoPd}(110)}$ and K_1^{CoPd} have different signs. This corresponds to the sign reversal in the dependence $K_{\text{eff}}^{\text{Pd}/\alpha\text{-Co}}(T)$ (Fig. 7a) for the synthesis of CoPd(110) crystallites in the Pd/α-Co(110) films. The constant $K_1^{\text{CoPd}} = -(1.6 \pm 0.4) \times 10^5$ erg/cm^3 agrees well with the value obtained from the dependence $K_{\text{eff}}^{\text{Pd}/\alpha\text{-Co}}$ (T = 650°C) (Fig. 7b) for the CoPd(001) films. Thus, within the experimental accuracy, for the epitaxial film systems CoPd(110) (Fig. 4b) and CoPd(001) (Fig. 6b), we obtained the same estimate for the first magnetocrystalline anisotropy constant of the disordered CoPd phase: $K_1^{\text{CoPd}} = -(1.6 \pm 0.4) \times 10^5$ erg/cm^3. However, this value is more than two times less than the value for bulk CoPd samples [38]. The reasons for the significant difference in the values of K_1^{CoPd} remain unclear.

In [39–53], it was shown that solid-state reactions in bilayer thin films start at minimum temperatures T_K of the solid phase structural transformation of the first phase ($T_{\text{in}} = T_K$) formed in the reaction products. For example, solid-state reactions in Pt/Co [39], Cu/Au [40], and Pd/Fe [41] films start at the order–disorder transition temperatures in the Pt–Co, Cu–Au, and Pd–Fe systems, whereas in Ni/Ti [42], Au/Cd [43], Al/Ni [44,45], and Mn/Fe [46] films, these reactions start at the reverse martensitic transition temperatures A_s in the Ni–Ti, Au–Cd, Al–Ni, and Mn–Fe systems, respectively. This rule also holds true for other structural transformations [47–53]. On this basis, we can assume the existence of a structural phase transition at a temperature of ~400°C in the region of the equiatomic composition of the Co–Pd system. This transition can be associated with the existence of the martensitic transition or the order–disorder transformation in the Co–Pd system.

It is known that, in pure Co and some alloys based on Co, such as Co–Ni, Co–Al, Co–Mn, Co–Ge, and Co–Cu, there occurs the martensitic transformation β ⟷ α [54–57]. For pure Co, the reverse martensitic transformation temperature A_s = 429–445°C [54] is close to the initiation temperature T_{in} of the solid-state reaction in polycrystalline Pd/Co films and epitaxial Pd/α-Co(110) and Pd/β-Co(001) films. This suggests the following scenario of the synthesis of the CoPd phase. An increase in the substrate temperature T above the reverse martensitic transformation temperature A_s ~ 400°C, the CoPd austenite phase is formed at the Pd/Co interface due to the migration of Pd atoms into polycrystalline Co or epitaxial layers of β-Co(001) and α-Co(110). However, a decrease in the substrate temperature to the liquid-nitrogen temperature does not cause a transition of the CoPd austenite phase to the CoPd martensite phase. This suggests either that the martensitic transformation in the CoPd alloy is suppressed or that the temperature A_s of the direct martensitic transition β ⟶ α is below –196°C. For example, in the Co–Ni system, the CoNi austenite phase transforms into the martensite phase upon cooling to the liquid-nitrogen temperature [54].

The solid-state synthesis of the CoPd alloy in Pd/Co films can also be determined by the order–disorder transition in the Co–Pd system. The $L1_0$ superstructure is not found in bulk samples of Co_xPd_{1-x}. However, according to some publications, the formation of the $L1_0$ superstructure was observed in Co/Pd(111) films at 560 K [10] and in CoPd films after annealing at 750°C [15]. Possibly, the difficulties encountered in the experimental determination of the $L1_0$ superstructure are associated with the very slow kinetics of atomic ordering in the CoPd alloy.

The above arguments do not give a clear answer to the question as to which solid-state transformation is associated with the synthesis of the CoPd alloy in Pd/Co films after annealings above ~400°C. However, certainly, the occurrence of chemical interactions between Pd and Co above 400°C, which lead to the breaking of chemical bonds, the mixing of Co and Pd layers, and the synthesis of the CoPd phase, indicates the existence of a structural transition in the Co–Pd system at a temperature of 400°C.

4. CONCLUSIONS

It was shown that, regardless of the structural modifications of cobalt, the solid-state reaction between the Co and Pd films begins to occur at the temperature T_{in} = 400°C and is fully completed at a temperature of 650°C with the formation of the disordered CoPd phase. For Pd/α-Co(110) and Pd/β-Co(001) bilayer films with the 1Co : 1Pd atomic composition, the synthesis of the CoPd alloy leads to different epitaxial relationships for the growth of CoPd crystallites on the MgO(001) substrate: CoPd(110)$\langle \bar{1}11 \rangle$ || MgO(001)⟨100⟩ and CoPd(001)[100] || MgO(001)[100], respectively. For the two epitaxial film systems, the estimation of the first magnetocrystalline anisotropy constants of the disordered CoPd phase gave the same value: $K_1^{\text{CoPd}} = -(1.6 \pm 0.4) \times 10^5$ erg/cm^3. Based on the analysis of the results of the investigations of the relationship between the solid-state reactions and transformations in film structures, it was assumed that the solid-state transformation occurs in the Co–Pd system at a temperature of ~400°C.

ACKNOWLEDGMENTS

We would like to thank L.A. Solov'ev for his assistance in performing the X-ray diffraction investigations of the epitaxial orientation of phases in Pd/α-Co(110) and Pd/β-Co(001) samples.

This study was supported in part by the Russian Foundation for Basic Research (project no. 15-02-00948).

REFERENCES

1. B. M. Lairson, W. Liu, A. P. Payne, C. Baldwin, and H. Hamilton, J. Appl. Phys. **77**, 6675 (1995).
2. B. D. Terris, J. Magn. Magn. Mater. **321**, 512 (2009).
3. S. Mangin, D. Ravelosona, J. A. Katine, M. J. Carey, B. D. Terris, and E. E. Fullerton, Nat. Mater. **5**, 210 (2006).
4. Z. Liu, R. Brandt, O. Hellwig, S. Florez, T. Thomson, B. Terris, and H. Schmidt, J. Magn. Magn. Mater. **323**, 1623 (2011).
5. D. Weller, A. Moser, L. Folks, M. E. Best, W. Lee, M. F. Toney, M. Schwickert, J.-U. Thiele, and M. F. Doerner, IEEE Trans. Magn. **36**, 10 (2000).
6. P. F. Carcia, A. D. Meinhaldt, and A. Suna, Appl. Phys. Lett. **47**, 178 (1985).
7. K. Yakushiji, T. Saruya, H. Kubota, A. Fukushima, T. Nagahama, S. Yuasa, and K. Ando, Appl. Phys. Lett. **97**, 232508 (2010).
8. H. Yamane, Y. Maeno, and M. Kobayashi, Appl. Phys. Lett. **62**, 1562 (1993).
9. M. Gottwald, K. Lee, J. J. Kan, B. Ocker, J. Wrona, S. Tibus, J. Langer, S. H. Kang, and E. E. Fullerton, Appl. Phys. Lett. **102**, 052405 (2013).
10. A. Murdoch, A. G. Trant, J. Gustafson, T. E. Jones, T. C. Q. Noakes, P. Bailey, and C. J. Baddeley, Surf. Sci. **608**, 212 (2013).
11. J. Carrey, A. E. Berkowitz, W. F. Egelhoff, and D. J. Smith, Appl. Phys. Lett. **83**, 5259 (2003).
12. L. F. Schelp, M. Carara, A. D. C. Viegas, M. A. Z. Vasconcellos, and J. E. Schmidt, J. Appl. Phys. **75**, 5262 (1994).
13. Ph. M. Leufke, S. Riedel, M.-S. Lee, J. Li, H. Rohrmann, Th. Eimüller, P. Leiderer, J. Boneberg, G. Schatz, and M. Albrecht, J. Appl. Phys. **105**, 113915 (2009).
14. J. M. MacLaren and R. H. Victora, J. Appl. Phys. **76**, 6069 (1994).
15. Y. Matsuo, J. Phys. Soc. Jpn. **32**, 972 (1972).
16. *Thin Films: Interdiffusion and Reaction*, Ed. by J. M. Poate, K. N. Tu, and J. W. Meyer (Wiley-Interscience, New York, 1978).
17. R. Pretorius, C. C. Theron, A. Vantomme, and J. W. Mayer, Crit. Rev. Solid State Mater. Sci. **24**, 1 (1999).
18. T. Laurila and J. Molarius, Crit. Rev. Solid State Mater. Sci. **28**, 185 (2003).
19. Yu. V. Goryunov, M. G. Khusainov, I. A. Garifullin, F. Schreiber, J. Pelzl, Th. Zeidler, K. Bröhl, N. Metoki, and H. Zabel, J. Magn. Magn. Mater. **138**, 216 (1994).
20. E. Gu, M. Gester, R. J. Hicken, C. Daboo, M. Tselepi, S. J. Gray, J. A. C. Bland, L. M. Brown, T. Thomson, and P. C. Riedi, Phys. Rev. B: Condens. Matter **52**, 14704 (1995).
21. J. F. Calleja, Y. Huttel, M. C. Contreras, E. Navarro, B. Presa, R. Matarranz, and A. Cebollada, J. Appl. Phys. **100**, 053917 (2006).
22. R. M. Bozorth, Phys. Rev. **96**, 311 (1954).
23. H. Sato, R. S. Toth, and R. W. Astrue, J. Appl. Phys. **34**, 1062 (1963).
24. O. Benamara, E. Snoeck, T. Blon, and M. Respaud, J. Cryst. Grown **312**, 1636 (2010).
25. M. J. M. Pires, A. A. C. Cotta, M. D. Martins, A. M. A. Silva, and W. A. A. Macedo, J. Magn. Magn. Mater. **323**, 789 (2011).
26. J. A. Wolf, J. J. Krebs, and G. A. Prinz, Appl. Phys. Lett. **65**, 1057 (1994).
27. M. Hashimoto, H. Qiu, T. Ohbuchi, M. Adamik, H. Nakai, A. Barna, and P. B. Barna, J. Cryst. Growth **166**, 792 (1996).
28. T. Suzuki, D. Weller, C.-A. Chang, R. Savoy, T. Huang, B. A. Gurney, and V. Speriosu, Appl. Phys. Lett. **64**, 2736 (1994).
29. O. Yabuhara, M. Ohtake, K. Tobari, T. Nishiyama, F. Kirino, and M. Futamoto, Thin Solid Films **519**, 8359 (2011).
30. J. R. Childress, J. L. Duvail, S. Jasmin, A. Barthélémy, A. Fert, A. Schuhl, O. Durand, and P. Galtier, J. Appl. Phys. **75**, 6412 (1994).
31. M. Wuttig, B. Feldmann, J. Thomassen, F. May, H. Zillgen, A. Brodde, H. Hannemann, and H. Neddermeyer, Surf. Sci. **291**, 14 (1993).
32. P. Schmailzl, K. Schmidt, P. Bayer, R. Döll, and K. Heinz, Surf. Sci. **312**, 73 (1994).
33. R. Naik, C. Kota, J. S. Payson, and G. L. Dunifer, Phys. Rev. B: Condens. Matter **48**, 1008 (1993).
34. F. Scheurer, R. Allenspach, P. Xhonneux, and E. Courtens, Phys. Rev. B: Condens. Matter **48**, 9890 (1993).
35. T. Bernhard, M. Baron, M. Gruyters, and H. Winter, Surf. Sci. **600**, 1877 (2006).
36. J. Shen, C. Schmidthals, J. Woltersdorf, and J. Kirschner, Surf. Sci. **407**, 90 (1998).
37. V. G. Myagkov, L. E. Bykova, and L. A. Solovyov, J. Magn. Magn. Mater. **322**, 1715 (2010).
38. N. Miyata, M. Hagiwara, Y. Ichiyanagi, K. Kuwahara, and H. Matsufuji, J. Phys. Soc. Jpn. **55**, 961 (1986).
39. V. G. Myagkov, L. A. Li, L. E. Bykova, I. A. Turpanov, P. D. Kim, G. V. Bondarenko, and G. N. Bondarenko, Phys. Solid State **42** (5), 968 (2000).
40. V. G. Myagkov, L. E. Bykova, V. S. Zhigalov, A. I. Pol'skii, and F. V. Myagkov, JETP Lett. **71** (5), 183 (2000).
41. V. G. Myagkov, V. S. Zhigalov, L. E. Bykova, L. A. Solov'ev, and G. N. Bondarenko, JETP Lett. **91** (9), 481 (2010).
42. V. G. Myagkov, L. E. Bykova, L. A. Li, I. A. Turpanov, and G. N. Bondarenko, Dokl. Phys. **47** (2), 95 (2002).
43. V. G. Myagkov, L. E. Bykova, and G. N. Bondarenko, Dokl. Phys. **48** (1), 30 (2003).

44. V. G. Myagkov and L. E. Bykova, Dokl. Phys. **49** (5), 289 (2004).
45. V. G. Myagkov, L. E. Bykova, S. M. Zharkov, and G. V. Bondarenko, Solid State Phenom. **138**, 377 (2008).
46. V. S. Zhigalov, V. G. Myagkov, O. A. Bayukov, L. E. Bykova, G. N. Bondarenko, and A. A. Matsynin, JETP Lett. **89** (12), 621 (2009).
47. V. G. Myagkov, L. E. Bykova, and G. N. Bondarenko, Dokl. Phys. **48** (5), 206 (2003).
48. V. G. Myagkov, V. C. Zhigalov, L. E. Bykova, and G. N. Bondarenko, J. Magn. Magn. Mater. **305**, 334 (2006).
49. V. G. Myagkov, V. C. Zhigalov, L. E. Bykova, G. V. Bondarenko, and G. N. Bondarenko, J. Magn. Magn. Mater. **310**, 126 (2007).
50. V. S. Zhigalov, V. G. Myagkov, L. A. Solov'ev, G. N. Bondarenko, and L. E. Bykova, JETP Lett. **88** (6), 389 (2008).
51. V. G. Myagkov, L. E. Bykova, G. N. Bondarenko, and V. S. Zhigalov, JETP Lett. **88** (8), 515 (2008).
52. V. G. Myagkov, O. A. Baykov, L. E. Bykova, and G. N. Bondarenko, J. Magn. Magn. Mater. **321**, 2260 (2009).
53. V. G. Myagkov, V. S. Zhigalov, A. A. Matsynin, L. E. Bykova, G. V. Bondarenko, G. N. Bondarenko, G. S. Patrin, and D. A. Velikanov, JETP Lett. **96** (1), 40 (2012).
54. H. Yang and Y. Liu, Acta Mater. **54**, 4895 (2006).
55. T. Omori, Y. Sutou, K. Oikawa, R. Kainuma, and K. Ishida, Mater. Trans. **44**, 2732 (2003).
56. W. Zhou, Y. Liu, B. Jiang, and P. Zhou, Mater. Sci. Eng., A **438–440**, 468 (2006).
57. T. Nishizawa and K. Ishida, Bull. Alloy Phase Diagram **4,** 387 (1983).

Translated by O. Borovik-Romanova